pagepress

European Journal of Histochemistry 2023; volume 67:3596

An *ex vivo* experimental system to track fluorescent nanoparticles inside skeletal muscle

Laura Calderan,[1] Flavia Carton,[1]* Ilaria Andreana,[2] Valeria Bincoletto,[2] Silvia Arpicco,[2] Barbara Stella,[2] Manuela Malatesta[1]

[1]Department of Neurosciences, Biomedicine and Movement Sciences, Anatomy and Histology Section, University of Verona; [2]Department of Drug Science and Technology, University of Turin, Italy

**Present address: Department of Health Sciences, University of Piemonte Orientale "A. Avogadro", Novara, Italy*

ABSTRACT

The development of novel nanoconstructs for biomedical applications requires the assessment of their biodistribution, metabolism and clearance in single cells, organs and entire organisms in a living environment. To reduce the number of *in vivo* experiments performed and to refine the methods used, in accordance with the 3Rs principle, this work proposes an *ex vivo* experimental system to monitor, using fluorescence microscopy, the distribution of nanoparticles in explanted murine skeletal muscle maintained in a bioreactor that can preserve the structural and functional features of the organ for long periods of time. Fluorescently-labelled liposomes and poly(lactide-co-glycolide) (PLGA)-based nanoparticles were injected into the intact soleus muscle (in the distal region close to the tendon) immediately after explants, and their distribution was analysed at increasing incubation times in cross cryosections from the proximal region of the belly. Both nanocarriers were clearly recognized in the muscle and were found to enter and migrate inside the myofibres, whereas their migration in the connective tissue seemed to be limited. In addition, some fluorescence signals were observed inside the macrophages, demonstrating the physiological clearance of the nanocarriers that did not enter the myofibres. Our *ex vivo* system therefore provides more information than previous in vitro experiments on cultured muscle cells, highlighting the need for the appropriate functionalization of nanocarriers if myofibre targeting is to be improved.

Key words: explanted muscle; intramuscular injection; liposomes; PLGA nanoparticles; bioreactor; fluorescence microscopy.

Correspondence: Prof. Manuela Malatesta, Department of Neurosciences, Biomedicine and Movement Sciences, Anatomy and Histology Section, University of Verona, Strada Le Grazie 8, 37134 Verona, Italy. Tel. +39.045.8027569. E-mail: manuela.malatesta@univr.it.

Contributions: L.C. and M.M. conceived the study and designed the experiments; L.C., F.C., I.A. and V.B. performed the experiments; L.C., F.C., S.A., B.S. and M.M. analysed and interpreted the results; L.C. and M.M. wrote the manuscript. All authors read and approved the final version of the manuscript and agreed to be accountable for all aspects of the work.

Funding: This work did not receive specific funding and was performed thanks to intramural funds to M.M.

Conflict of interest: The authors declare that they have no competing interests.

Availability of data and materials: The data analysed in this study are available from the corresponding author upon reasonable request.

Ethics approval: This study was approved by the Italian Ministry of Health (protocol code: 56DC9.N.7O3).

Introduction

The development of novel nanoconstructs that are intended for biomedical applications requires initial physico-chemical and pharmacological characterization. In order to assess their biodistribution, clearance and relationships with cell and tissue constituents, the nanoconstructs must then be administered in a living environment to single cells, organs or entire organisms. While no ethical issue exists in the use of cultured cells, especially when established cell lines are used, tests on organs and organisms imply the use of laboratory animals, which entails significant ethical concerns. In accordance with the principles of the 3Rs (Replacement, Reduction and Refinement),[1] the nanomedicine field has invested a great deal of effort in replacing *in vivo* experiments with *in vitro* systems where possible (recent review in[2]), thus reducing the number of animals needed to obtain the relevant information. However, while currently available *in vitro* systems, including microfluidic technology,[3,4] have proven to be reliable for basic and early-phase applied research, they are still unable to reproduce the structural and functional complexity of the living milieu.

A relatively easy compromise between *in vivo* and *in vitro* systems can be found in *ex vivo* models; surgical and bioptic explants from humans and animals, as well as from biological material that is discarded from control animals in any experimental protocol, may be used for scientific aims, drastically reducing the need for specific *in vivo* tests. Although the structural and functional preservation of explanted organs and tissues in culture is obviously limited, bioreactors can provide fluid dynamics that mimic physiological conditions, leading to significant advancements in the reliability of *ex vivo* models, even for long-term studies.[5-9]

Our research group has long studied the suitability of different types of nanovectors for the delivery of therapeutic agents to muscle cells with the aim of treating still incurable muscular disorders (*e.g.,* myotonic dystrophy, age-related atrophy), and cultured muscle cells have always been used to assess the uptake, biocompatibility and efficacy of the nanoparticles (NPs) used.[10-15] However, skeletal muscle is a composite organ made up of muscle cells, but also of connective tissue, blood vessels and nerves, meaning that the NPs intended for intramuscular delivery are required to move though this complex environment before finally entering the myofibres. We have therefore set up an *ex vivo* experimental system to monitor the biodistribution of fluorescently-labelled lipid and polymeric NPs injected into explanted murine skeletal muscle that was maintained in a bioreactor under dynamic conditions.

Materials and Methods

NP preparation and characterisation

Fluorescently labelled liposomes were prepared by the thin lipid film hydration and extrusion method, as previously described.[10] Briefly, a lipid film composed of 1,2-dipalmitoyl-*sn*-glycero-3-phosphocholine, cholesterol and L-α phosphatidyl-DL-glycerol sodium salt (Merck, Darmstadt, Germany), in a 70:30:3 molar ratio, was hydrated with a 10 mM solution of fluorescein-5-(and-6)-sulfonic acid trisodium salt (Invitrogen, Life Technologies, Carlsbad, CA, USA) in HEPES (4-[2-hydroxyethyl] piperazine-1-ethanesulforic acid) buffer (pH 7.4), and the suspension was extruded (Extruder, Lipex, Northern Lipids Inc., Vancouver, Canada) at 60°C, by passing the suspension ten times through 400 and 200 nm polycarbonate membranes (Costar, Corning Inc., Corning, NY, USA) under nitrogen. Liposomes were purified through chromatography on Sepharose CL-4B columns, eluting with HEPES buffer. Fluorescently labelled poly(lactide-*co*-glycolide) (PLGA) NPs were prepared using the nanoprecipitation technique.[16] Briefly, 6 mg of PLGA 75:25 (Resomer® RG 752H, Merck) and 8.4 µg of Nile red (9-diethylamino-5H-benzo[α]phenoxazine-5-one, Merck) were co-dissolved in 1 mL of acetone. This organic solution was then poured into 2 mL of MilliQ® water under magnetic stirring. Particle precipitation occurred spontaneously. Acetone was then evaporated under reduced pressure to provide an aqueous suspension of fluorescent NPs that were purified from the non-incorporated dye *via* gel filtration on a Sepharose CL-4B column, eluting with MilliQ® water.

The mean particle size and polydispersity index (PDI) of the liposomes and PLGA NPs were determined at 25°C by quasi-elastic light scattering (QELS) using a nanosizer (Nanosizer Nano Z, Malvern Inst., Malvern, PA, USA). The selected angle was 173° and the measurements were made after the 1/10 dilution of the NP suspensions in MilliQ® water.

The particle surface charge of the NPs was investigated *via* zeta potential measurements at 25°C using the Nanosizer Nano Z and the Smoluchowski equation after the suspensions were diluted in MilliQ® water.

Size, PDI and zeta potential measurements were performed in triplicate.

Muscle isolation

Soleus muscles were explanted from control (untreated) 3-month-old male Balb/c mice that were sacrificed as part of a research project approved by the Italian Ministry of Health (protocol code: 56DC9.N.7O3). The mice were sacrificed *via* carbon oxide overdose in a pre-anaesthesia chamber and then, after ensuring the absence of respiration and pain reaction from hind-paw stimulation, we proceeded with cervical dislocation. The soleus muscle was isolated and carefully excised from each paw, paying attention to preserve both tendons and not to damage the integrity of muscle belly. Two soleus muscles per experimental condition were used. As previously reported,[6] the freshly excised muscles were rapidly washed in warm culture medium composed of medium 199 (Gibco, Waltham, MA, USA) supplemented with 5.5 mM glucose, 2.54 mM $CaCl_2$ (Merk), 25 mM $NaHCO_3$, 0.6 nM insulin (Sigma-Aldrich, St. Louis, MO, USA), 0.1% bovine serum albumin (Gibco), 200 µU/mL penicillin-streptomycin (Gibco) and 0.5% amphotericin B (Gibco).

NP injection and muscle incubation in the bioreactor

Immediately after excision, after the wash in pre-warmed medium, the muscles were placed on a horizontal plane and 5 µL of nanocarrier suspension were injected *via* the horizontal insertion, parallel to the longitudinal axis and the surface of the muscle belly, of a 10 µL/Microliter™ Syringe 23S/171"/2 (Hamilton Central Europe srl, Giarmata, Romania) into the distal end (Figure 1). Fluorescent liposomes were administered at the concentration of 5 mg/mL in HEPES buffer, while PLGA NPs were administered at the concentration of 3 mg PLGA/mL of MilliQ® water.

After injection, the muscles were placed into a bioreactor (IV-Tech). Specifically, each muscle was placed into a culture chamber (LiveBox1) containing 1.5 mL of medium. Four chambers were joined in parallel in a fluidic circuit connected to four 15 mL mixing chambers and a peristaltic pump LiveFlow (IV-Tech). A flow rate of 300 µL/min was applied. The bioreactor was maintained in an incubator at 37°C in a 5% CO_2 humidified atmosphere, and the muscles were incubated for 1 h, 3 h, 6 h and 24 h under fluid dynamic conditions.

Muscle processing for fluorescence microscopy analysis

The samples were processed for fluorescence microscopy to evaluate the distribution of the injected NPs within the muscles at each incubation time.

The muscles were cut crosswise into two halves (proximal and distal), which were immersed in isopentane that had been pre-cooled in liquid nitrogen for 30 s to allow for complete freezing, and were then kept at -80°C. For sectioning, the samples were embedded in optimal cutting temperature (OCT) compound (Sigma-Aldrich), and 10 µm-thick cross sections were cut in a cryostat and collected on glass slides. For the fluorescence microscopy observations, cryosections were hydrated for 5 min in PBS, weakly stained with either trypan blue (Sigma-Aldrich), diluted 1:10 in PBS for 30 s (if treated with liposomes), or with fluorescein-5-isothiocyanate (FITC, Sigma-Aldrich) (0.2 mg/mL PBS) for 1 min (if treated with PLGA NPs), counterstained with Hoechst 33342 (0.5 µg/mL PBS) for 5 min and finally mounted in a mixture of PBS/glycerol (1:1). The sections were observed on an Olympus BX51 microscope equipped with a 100W mercury lamp under the following conditions: 450-480 nm excitation filter (excf), 500 nm dichroic mirror (dm) and 515 nm barrier filter (bf), for FITC; 540 nm excf, 580 nm dm, and 620 nm bf, for Nile red and trypan blue; 330-385 nm excf, 400 nm dm, and 420 nm bf, for Hoechst 33342. Images were recorded using an QICAM Fast 1394 digital camera (QImaging) and processed using Image-Pro Plus 7.0 software (Media Cybernetics Inc., Bethesda, MD, USA).

Results and Discussion

In this study, soleus muscles explanted from mice and maintained in culture under fluid dynamic conditions were used as an *ex vivo* model to investigate the biodistribution of lipid and polymer NPs administered by intramuscular injection. The soleus muscle was chosen because its isolation and excision are relatively simple thanks to the proximal slender tendon at the head of the fibula and the distal Achilles tendon (shared with the gastrocnemius muscle) at the tuber calcanei. Moreover, it had already been found that the structural features of the soleus muscle are excellently preserved for up to 48 h in the bioreactor used in this study.[6]

The injection was performed using a Hamilton microsyringe to minimize tissue damage and precisely modulate the dosage. In addition, to distinguish NP diffusion due to the forced, massive injection from their distribution in the muscle parenchyma far from the inoculation site, NPs were injected into the distal end of the muscle belly and their distribution within the muscle was monitored in the cross cryosections obtained from the proximal half of the belly.

Liposomes and PLGA NPs were used for intramuscular administration as they have been proven to be biocompatible and capable of entering muscle cells – both cycling myoblasts and terminally differentiated myotubes – *in vitro*.[10,11] In particular, the mean sizes of liposomes and PLGA NPs in this study were around 180 nm and 120 nm, respectively, with a PDI of below 0.085. The zeta potential value was around -16 mV for liposomes and -48 mV for PLGA NPs (Table 1).

Both types of nanocarrier efficiently incorporated the fluorescent dyes. Specifically, the encapsulation efficiency of the hydrophilic fluorescein-based dye into liposomes was 90%, while the association rate for the highly lipophilic dye Nile Red was 95% for PLGA NPs. As demonstrated in previous studies,[10,11,16,17] the fluorescent dyes were stably associated to the nanocarriers.

Fluorescence microscopy observations showed that liposomes and PLGA NPs underwent similar intramuscular distribution. In fact, 1 h after administration, very large amounts of both nanocarriers were found in the distal muscle region, close to the site of injection (Figures 2a and 3a), whereas they were not found in the proximal region (*not shown*). After 3 h of incubation, both liposomes and PLGA NPs were observed in the proximal region in low numbers. The liposomes were detected almost exclusively inside the myofibres (Figure 2b), whereas PLGA NPs were confined to the connective tissue (Figure 3b). After 6 h and 24 h of incubation, the amount of liposomes inside myofibres remained very low (Figure 2 c,d). In the connective tissue, some macrophages showed a green fluorescent signal in their cytoplasm, while the liposomes were barely present in the extracellular matrix (Figure 2c). Conversely, PLGA NPs became progressively more numerous inside the myofibres from 6 to 24 h of incubation (Figure 3 c,d); they were also internalised by macrophages (Figure 3d), although they rarely occurred in the extracellular matrix of the connective tissue.

These observations appear to demonstrate that migration to the connective tissue is limited for both nanocarriers. The presence of

Table 1. Physico-chemical characteristics (mean diameter, PDI and zeta potential) of liposomes and PLGA NPs (n=3).

Nanosystem type	Mean diameter (nm ± SD)	PDI	Zeta potential (mV ± SD)
Liposomes	180±1	0.084	-16.5±1.1
PLGA NPs	117±2	0.076	-48.5±1.8

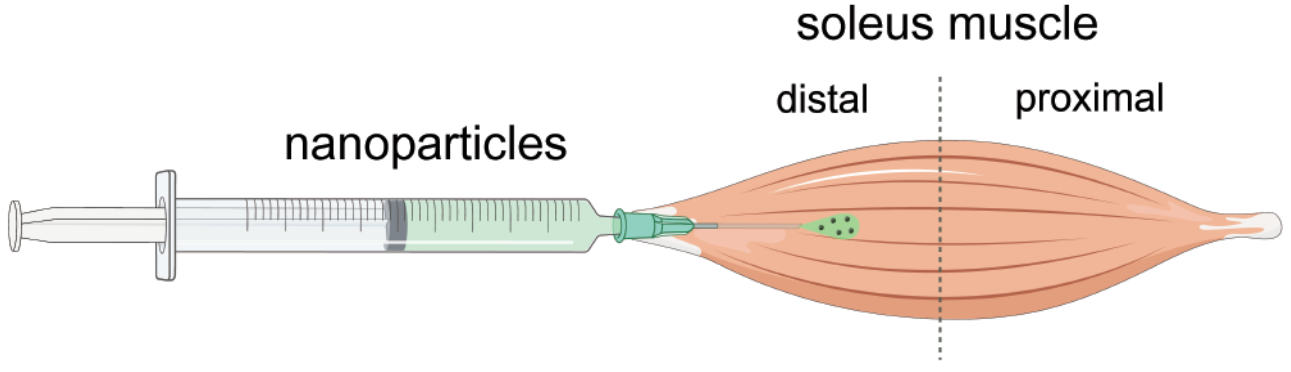

Figure 1. Schematic illustration of the *ex vivo* injection of nanocarriers into the explanted soleus muscle.

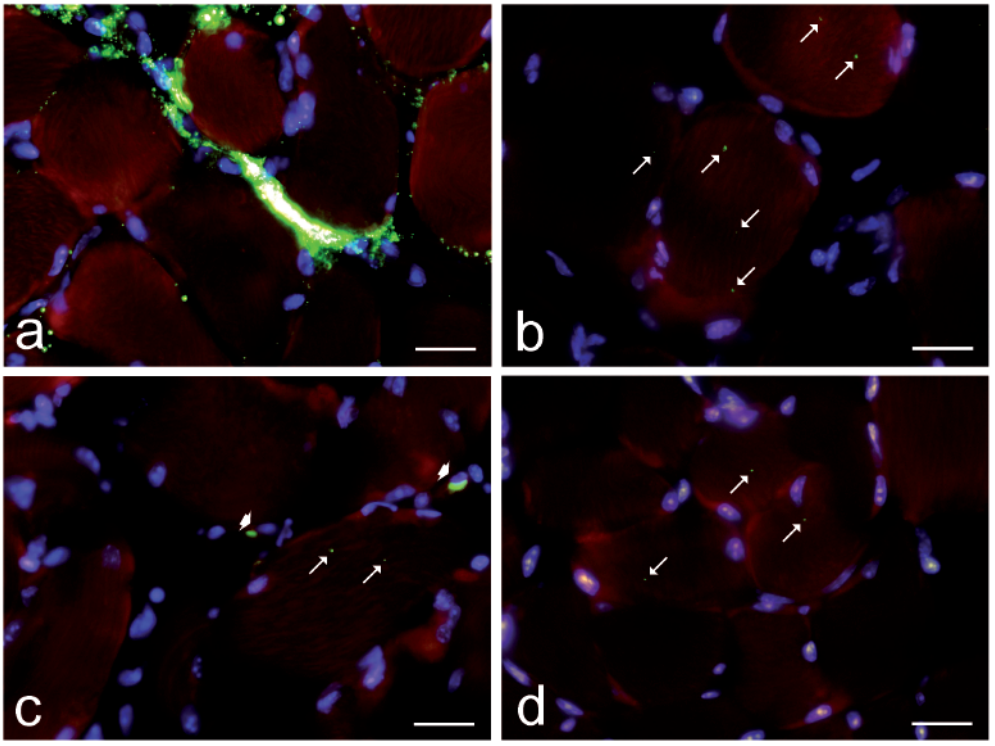

Figure 2. Soleus muscle, intramuscular injection of FITC-labelled liposomes: trypan blue staining, nuclei counterstaining with Hoechst 33342. a) Distal region 1 h after injection: a huge number of liposomes are present in the connective tissue among the myofibres. Proximal region 3 h (b), 6 h (c) and 24 h (d) after injection: only a small number of liposomes (arrows) are present inside the myofibres. Note the fluorescent signal inside the macrophages (arrowheads in c). Scale bars: 25 µm.

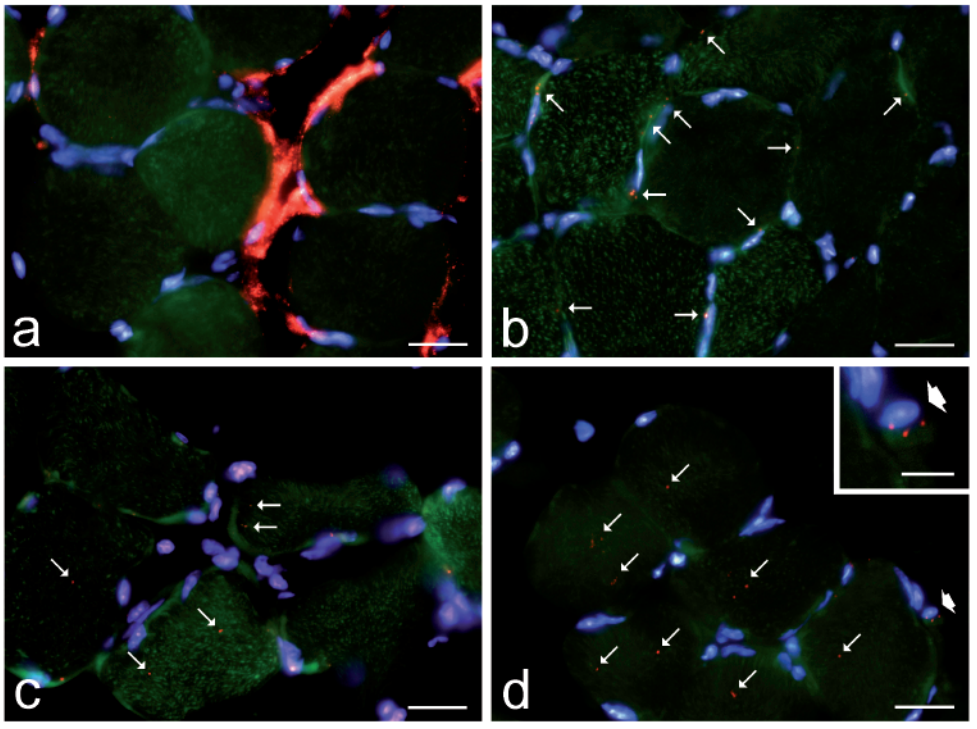

Figure 3. Soleus muscle, intramuscular injection of Nile red-labelled PLGA NPs: FITC staining, nuclei counterstaining with Hoechst 33342. a) Distal region 1 h after injection: a huge number of NPs are present in the connective tissue among the myofibres. b) Proximal region 3 h after injection: the NPs (arrows) are confined to the connective tissue surrounding the myofibres. c) Proximal region 6 h after injection: a few NPs (arrows) are present inside the myofibres. d) Proximal region 24 h after injection: NPs (arrows) are present inside the myofibres and macrophages (arrowhead, high magnification in the inset). Scale bars: 25 µm; inset bar: 10 µm.

NPs in the myofibres in the proximal muscle end and the absence of NPs in the connective tissue suggests that both the liposomes and PLGA NPs are able to enter the myofibres and migrate inside them. In fact, the presence of the nanocarriers was very low in the connective tissue in the proximal muscle region 6 h after injection, whereas a fluorescence signal was often observed inside macrophages, thus demonstrating the physiological clearance of the liposomes and PLGA NPs that did not enter the myofibres. It is likely that the three-dimensional network of fibrous proteins in the extracellular connective matrix entraps the nanocarriers due to steric and chemical interactions, allowing macrophages to easily phagocytose them. The occurrence of macrophages that phagocytose the NPs 6 h and 24 h post-injection suggests that fluid dynamic conditions preserve not only the structure, but also the functions of the cellular components of the explanted skeletal muscle. The fluid dynamic environment certainly facilitates molecular turnover and thus improves both oxygen/nutrient supply and catabolite removal,[6,11] while it is known that the metabolism of skeletal muscle is especially sensitive to variations in flow rate.[18]

Liposomes were proven to rapidly enter myofibres and migrate inside the sarcoplasm as they were already observed in the proximal region of the muscle after 3 h post-injection. However, their number remained very low until 24 h post-injection. This is consistent with previous observations in cultured muscle cells[10,11] and non-muscular cells,[17] demonstrating that chemical affinity with the cell membrane favours the easy uptake of these lipid nanocarriers. Nevertheless, once in the cytoplasm, they are rapidly degraded by endogenous enzymes, which prevent their accumulation.

On the other hand, PLGA NPs seem to take longer to enter myofibres than the liposomes since the few PLGA NPs observed in the proximal region after 3 h were confined to the connective tissue. However, they progressively accumulated inside the myofibres starting from 6 h post-incubation. Again, this behaviour is consistent with our observations in muscle cells *in vitro*,[10,11] where PLGA NPs cross the plasmalemma through endocytosis, escape endosomes and accumulate in the cytoplasm, although they re-enter the lytic pathway *via* autophagocytic processes, thus preventing excessive storage and consequent cell stress and damage.

In summary, our experimental *ex vivo* model has allowed us to expand the sum of knowledge on the suitability of liposomes and PLGA NPs for skeletal muscle administration, and has confirmed their ability to enter muscle cells, but also highlights their limitations in crossing the connective tissue barrier once inside the complex histological architecture of skeletal muscles. This suggests that appropriate nanocarrier functionalization would improve targeting to myofibres, and experiments are in progress in our laboratories on this subject.

We cannot exclude the possibility that the intramuscular distribution of NPs may also be affected by a lack of muscle contraction, which influences structural, molecular and metabolic features,[19] and is obviously lost in the bioreactor.

Explanted skeletal muscle that is maintained under fluid dynamic conditions is a suitable and handy *ex vivo* model for testing nanocarriers intended for muscular use; the labelling of nanocarriers with fluorescent molecules makes them easily recognizable with a conventional fluorescence microscope, the muscle can be rapidly and easily processed using cryofixation and cryosectioning, and, except for routine tissue and nuclei counterstaining, no specific staining is required to observe the samples. This *ex vivo* system may therefore be envisaged as an intermediate step between early *in vitro* and final *in vivo* analyses, enabling the study of the intramuscular biodistribution of nanoconstructs in the morpho-functional unit that is composed of skeletal muscle tissue and connective tissue. Last, but not least, this new approach brings with it positive ethical and economic implications for research activity.

Acknowledgments

We thank Dr. Dale James Matthew Lawson for English language copyediting.

References

1. Russell WMS, Burch RL. The principles of humane experimental technique. London, R-U, Universities Federation for Animal Welfare; 1959.
2. Carton F, Malatesta M. In vitro models of biological barriers for nanomedical research. Int J Mol Sci 2022;23:8910.
3. Bhatia SN, Ingber E. Microfluidic organs-on-chips. Nat Biotechnol 2014;32:760-72.
4. Niculescu AG, Chircov C, Bîrcă AC, Grumezescu AM. Fabrication and applications of microfluidic devices: A review. Int J Mol Sci 2021;22:2011.
5. Ferrarini M, Steimberg N, Ponzoni M, Belloni D, Berenzi A, Girlanda S, et al. Ex-vivo dynamic 3-D culture of human tissues in the RCCS™ bioreactor allows the study of Multiple Myeloma biology and response to therapy. PLoS One 2013;8:e71613.
6. Carton F, Calderan L, Malatesta M. Incubation under fluid dynamic conditions markedly improves the structural preservation in vitro of explanted skeletal muscles. Eur J Histochem 2017;61:2862.
7. Wunderli SL, Widmer J, Amrein N, Foolen J, Silvan U, Leupin O, et al. Minimal mechanical load and tissue culture conditions preserve native cell phenotype and morphology in tendon-a novel ex vivo mouse explant model. J Orthop Res 2018;36:1383-90.
8. Cappellozza E, Zanzoni S, Malatesta M, Calderan L. Integrated microscopy and metabolomics to test an innovative fluid dynamic system for skin explants in vitro. Microsc Microanal 2021;27:923-34.
9. Cappellozza E, Boschi F, Sguizzato M, Esposito E, Cortesi R, Malatesta M, et al. A spectrofluorometric analysis to evaluate transcutaneous biodistribution of fluorescent nanoparticulate gel formulations. Eur J Histochem 2022;66:3321.
10. Costanzo M, Vurro F, Cisterna B, Boschi F, Marengo A, Montanari E, et al. Uptake and intracellular fate of biocompatible nanocarriers in cycling and noncycling cells. Nanomedicine (Lond) 2019;14:301-16.
11. Guglielmi V, Carton F, Vattemi G, Arpicco S, Stella B, Berlier G, et al. Uptake and intracellular distribution of different types of nanoparticles in primary human myoblasts and myotubes. Int J Pharm 2019;560:347-56.
12. Carton F, Repellin M, Lollo G, Malatesta M. Alcian blue staining to track the intracellular fate of hyaluronic-acid-based nanoparticles at transmission electron microscopy. Eur J Histochem 2019;63:3086.
13. Andreana I, Repellin M, Carton F, Kryza D, Briançon S, Chazaud B, et al. Nanomedicine for gene delivery and drug repurposing in the treatment of muscular dystrophies. Pharmaceutics 2021;13:278.
14. Costanzo M, Esposito E, Sguizzato M, Lacavalla MA, Drechsler M, Valacchi G, et al. Formulative study and intracellular fate evaluation of ethosomes and transethosomes for vitamin D3 delivery. Int J Mol Sci 2021;22:5341.
15. Repellin M, Carton F, Lollo G, Malatesta M. Alcian blue staining to visualize intracellular hyaluronic acid-based nanoparticles. Methods Mol Biol 2023;2566:313-20.
16. Fessi H, Puisieux F, Devissaguet JP, Ammoury N, Benita S.

Nanocapsule formation by interfacial polymer deposition following solvent displacement. Int J Pharm 1989;55:R1-R4.
17. Costanzo M, Carton F, Marengo A, Berlier G, Stella B, Arpicco S, et al. Fluorescence and electron microscopy to visualize the intracellular fate of nanoparticles for drug delivery. Eur J Histochem 2016;60:2640.
18. Korthuis RJ. Skeletal muscle circulation. San Rafael: Morgan & Claypool Life Sciences; 2011.
19. Franchi MV, Reeves ND, Narici MV. Skeletal muscle remodeling in response to eccentric vs. concentric loading: morphological, molecular, and metabolic adaptations. Front Physiol 2017;8:447.

Received for publication: 7 November 2022. Accepted for publication: 14 December 2022.

European Journal of Histochemistry 2023; 67:3596
doi:10.4081/ejh.2023.3596